Resolution of prestack seismic migration

Luděk Klimeš
Department of Geophysics, Charles University, Ke Karlovu 3, 121 16 Praha 2, Czech Republic, Fax: +420-2-2191 1214, E-mail: klimes@seis.karlov.mff.cuni.cz

Summary

Explicit approximate equations describing the physical meaning of the migrated sections are derived. The imaged combination of elastic parameters (reflectivity) depends on the selection of the polarizations of the incident and back–propagated wavefields and on the directions of propagation. The migrated section is then approximately the convolution of the unknown exact reflectivity with the resolution function depending on the aperture and on the form of the imaging time function.

Keywords

Elastic waves, macro–models, seismic migration, wavefield inversion, resolution.

1 Introduction

A general formulation of *prestack migration* based on imaging (mapping) incident and scattered wavefields, extrapolated into the macro–model by arbitrary numerical methods (Claerbout 1971) is considered in this paper. A *common shot* prestack migration is assumed since it is the most natural configuration from the physical point of view, although the same approach could simply be applied to other configurations. The presented theory is developed for *3-D elastic migrations* in 3-D elastic macro–models. Neither scalar acoustic wavefields nor 2-D migrations are separately investigated.

The goal of this paper is to study the physical meaning and spatial resolution of the migrated images.

Although the migrations are mostly performed in the isotropic macro–models, we shall present the equations in a general form suitable for elastic anisotropic models everywhere, where the assumption of isotropic models or perturbations enable for no considerable simplification of the theory. The equations expressed in terms of general stiffness matrix c_{ijkl} are often more concise and clear than the analogous explicit isotropic equations.

2 Notation

The geological structure is described in terms of the unknown material parameters

$$\varrho = \varrho(\mathbf{x}) \ , \quad c_{ijkl} = c_{ijkl}(\mathbf{x}) \quad . \tag{1}$$

The seismic macro–model of the geological structure is described in terms of the material parameters

$$\tilde{\varrho} = \tilde{\varrho}(\mathbf{x}) \ , \quad \tilde{c}_{ijkl} = \tilde{c}_{ijkl}(\mathbf{x}) \quad . \tag{2}$$

Difference between the geological structure and the model is

$$\Delta\varrho = \varrho - \tilde{\varrho} \ , \quad \Delta c_{ijkl} = c_{ijkl} - \tilde{c}_{ijkl} \quad . \tag{3}$$

In: Seismic Waves in Complex 3-D Structures, Report 6 (Department of Geophysics, Charles University, Prague, September 1997), revised November 1999

Seismic wavefield $u_i(\mathbf{x},t)$ in the geological structure is, approximately, subject to the elastodynamic equation

$$\varrho\ddot{u}_i = [c_{ijkl}u_{k,l}]_{,j} \quad , \tag{4}$$

where the partial derivatives are denoted in the following manner

$$f_{m,n} = \frac{\partial f_m}{\partial x_n} \ , \quad \dot{f}_m = \frac{\partial f_m}{\partial t} \quad . \tag{5}$$

Seismic wavefield $\tilde{u}_i(\mathbf{x},t)$ calculated for the same source in the macro–model is subject to the elastodynamic equation

$$\tilde{\varrho}\ddot{\tilde{u}}_i = [\tilde{c}_{ijkl}\tilde{u}_{k,l}]_{,j} \quad . \tag{6}$$

The Green tensor in the macro–model is defined by

$$\tilde{\varrho}(\mathbf{x})\ddot{G}_{im}(\mathbf{x},t,\mathbf{x}',t') = [\tilde{c}_{ijkl}(\mathbf{x})G_{km,l}(\mathbf{x},t,\mathbf{x}',t')]_{,j} + \delta_{im}\,\delta(\mathbf{x}-\mathbf{x}')\,\delta(t-t') \quad , \tag{7}$$

where the partial derivatives are related to variables $\mathbf{x}$ and t.

3 Migration

In our approach, migration may be decomposed into following steps (Claerbout 1971):

(a) *extrapolation* of the wavefields from the source and receiver points into the macro–model, (b) *decomposition* of the extrapolated wavefields into waves of different properties, (b) *imaging* the extrapolated and decomposed wavefields.

3.1 Extrapolation

Assume that the seismic wavefield $u_i(\mathbf{x},t)$ is recorded at the receivers covering the "receiver area" along the Earth surface with a sufficient density to allow for the back–propagation of the recorded wavefield into the model.

Let us denote by $U_i(\mathbf{x},t)$ the "scattered" wavefield

$$\Delta u_i = u_i - \tilde{u}_i \quad , \tag{8}$$

back–propagated from the receiver area into the seismic macro–model.

The approximate incident wavefield $\tilde{u}_i(\mathbf{x},t)$ and the back–propagated wavefield $U_i(\mathbf{x},t)$ may be calculated in the model $\tilde{\varrho}(\mathbf{x})$, $\tilde{c}_{ijkl}(\mathbf{x})$ by any convenient numerical method.

3.2 Decomposition

To resolve more than a single linear combination of material perturbations (3), it is desirable to attempt to decompose both the approximate incident wavefield $\tilde{u}_i(\mathbf{x},t)$ and the back–propagated wavefield $U_i(\mathbf{x},t)$ at each point $\mathbf{x}$ locally into P and S waves or, better, into P waves and two polarizations of S waves. Such a decomposition may conveniently be accomplished by a proper choice of imaging functionals, see Section 6.

In addition, if the waves incident from considerably different directions can locally be distinguished in the approximate incident wavefield $\tilde{u}_i(\mathbf{x},t)$ or back–propagated wavefield $U_i(\mathbf{x},t)$, the respective wavefield should be decomposed into the parts corresponding to the different propagation directions, particularly for the purposes of the "amplitude–versus–angle" analysis.

If the decomposition into the parts corresponding to the different propagation directions is not possible, the amplitude–versus–angle analysis may be enabled by splitting the receiver area into two or more smaller receiver areas, e.g., by means of application of the aperture filter $a(\mathbf{x})$ dependent on the receiver positions $\mathbf{x}$. Such a splitting, however, deteriorates the lateral spatial resolution of the migrated sections.

If any of the above decompositions is applicable, let $\tilde{u}_i(\mathbf{x}, t)$ denote hereinafter one selected part of the decomposed approximate incident wavefield and $U_i(\mathbf{x}, t)$ one selected part of the back–propagated wavefield.

3.3 Imaging

Now we have, at each point $\mathbf{x}$, time functions $\tilde{u}_i(\mathbf{x}, t)$ and $U_i(\mathbf{x}, t)$.

Assume to have "imaging functional" (mapping procedure)

$$M(\bullet, \bullet): \quad \tilde{u}_i, U_i \longrightarrow m = M(\tilde{u}_i, U_i) \quad , \tag{9}$$

mapping the pair of functions $\tilde{u}_i = \tilde{u}_i(t)$ and $U_i = U_i(t)$ onto the real or complex numbers.

The *migrated section* is then

$$m(\mathbf{x}) = M\left(\tilde{u}_i(\mathbf{x}, \bullet), U_i(\mathbf{x}, \bullet)\right) \quad . \tag{10}$$

Here $f(\mathbf{x}, \bullet)$ stands for function

$$f(\mathbf{x}, \bullet): \quad t \longrightarrow f(\mathbf{x}, t) \quad . \tag{11}$$

4 Born approximation of the back–propagated scattered wavefield

Subtracting equation (6) from (4) we arrive at

$$\tilde{\varrho}\Delta\ddot{u}_i = [\tilde{c}_{ijkl}\Delta u_{k,l}]_{,j} - \Delta\varrho\ddot{\tilde{u}}_i + [\Delta c_{ijkl}\tilde{u}_{k,l}]_{,j} - \Delta\varrho\Delta\ddot{u}_i + [\Delta c_{ijkl}\Delta u_{k,l}]_{,j} \quad . \tag{12}$$

Neglecting the last two terms which are of the second order, we may express scattered wavefield $\Delta u(\mathbf{x}, t)$ in the form of the first–order Born approximation

$$\Delta u_i(\mathbf{x}, t) \approx \int\!\mathrm{d}\mathbf{x}'\!\int\!\mathrm{d}t'\; \tilde{G}_{im}(\mathbf{x}, t, \mathbf{x}', t')\left\{-\Delta\varrho(\mathbf{x}')\ddot{\tilde{u}}_m(\mathbf{x}', t') + [\Delta c_{mjkl}(\mathbf{x}')\tilde{u}_{k,l}(\mathbf{x}', t')]_{,j}\right\} \quad . \tag{13}$$

Assuming the boundaries of the integration domain sufficiently distant from the target zone, equation (13) is equivalent to

$$\Delta u_i(\mathbf{x}, t) \approx \int\!\mathrm{d}\mathbf{x}'\!\int\!\mathrm{d}t'$$
$$\times\Big[\dot{\tilde{G}}_{im}(\mathbf{x}, t, \mathbf{x}', t')\Delta\varrho(\mathbf{x}')\dot{\tilde{u}}_m(\mathbf{x}', t') - \tilde{G}_{im,j}(\mathbf{x}, t, \mathbf{x}', t')\Delta c_{mjkl}(\mathbf{x}')\tilde{u}_{k,l}(\mathbf{x}', t')\Big] \;, \tag{14}$$

where the partial derivatives are related to variables $\mathbf{x}'$ and t'.

We shall now, at least locally, apply the ray theory. Let $\gamma = (\gamma_1, \gamma_2) \in \Gamma$ be the angular directions of the slowness vectors $P_k(\mathbf{x}', \gamma)$ incident at point $\mathbf{x}'$ from the receiver area. Here Γ is the angular domain (aperture) corresponding to all rays arriving from the receiver area. The ray approximation of the Green tensor corresponding to a particular polarization is then

$$\tilde{G}_{im}(\mathbf{x}, t, \mathbf{x}', t') \approx \sqrt{\frac{\mathrm{d}\Gamma}{\mathrm{d}S}}\;\; \frac{E_i(\mathbf{x}, \gamma)E_m(\mathbf{x}', \gamma)T(\mathbf{x}, \mathbf{x}')}{4\pi\sqrt{\tilde{\varrho}(\mathbf{x})\tilde{v}(\mathbf{x})\tilde{\varrho}(\mathbf{x}')[\tilde{v}(\mathbf{x}')]^3}}\; \delta(t - \tau(\mathbf{x}, \mathbf{x}') - t') \;, \tag{15}$$

where E_K are the polarization vectors, $\tilde{v}$ is the phase velocity and $\mathrm{d}S$ is the cross section of the ray tube of angular size $\mathrm{d}\Gamma$, measured along the wavefront. Here $T(\mathbf{x},\mathbf{x}')$ is the accumulated reciprocal transmission coefficient describing amplitude losses between points $\mathbf{x}'$ and $\mathbf{x}$ due to attenuation and due to reflections and scattering into directions leading outside the vicinity of point $\mathbf{x}$. In an ideal case, $T(\mathbf{x},\mathbf{x}')\approx 1$. Possible phase shifts due to caustics will be annulled during the back–propagation and are thus not considered in (15).

The infinitesimal Green tensor $\mathrm{d}G_{im}$ back–propagated from a small wavefront element $\mathrm{d}S$, situated at point $\mathbf{x}''$, towards point $\mathbf{x}$, situated close to point $\mathbf{x}'$, may be evaluated using the representation theorem,

$$\mathrm{d}G_{im}(\mathbf{x},t,\mathbf{x}',t') \approx \mathrm{d}S\int \mathrm{d}t''\ \tilde{v}(\mathbf{x}'')P_j(\mathbf{x}'',\gamma)\tilde{c}_{njkl}(\mathbf{x}'')$$
$$\times\Big[-\tilde{G}_{ni}(\mathbf{x}'',t'',\mathbf{x},t)\tilde{G}_{km,l}(\mathbf{x}'',t'',\mathbf{x}',t') + \tilde{G}_{ki,l}(\mathbf{x}'',t'',\mathbf{x},t)\tilde{G}_{nm}(\mathbf{x}'',t'',\mathbf{x}',t')\Big]\ , \qquad (16)$$

where the partial derivatives are related to variables $\mathbf{x}''$ and t''. Equation (16) has been obtained by multiplying equation (7) for $\tilde{G}_{ki}(\mathbf{x}'',t'',\mathbf{x},t)$ by $\tilde{G}_{km}(\mathbf{x}'',t'',\mathbf{x}',t')$ and vice versa, and integrating the difference over volume inside a wavefront and over all times. The integral over the volume has then been converted using the Green theorem into the integral over the wavefront composed of elements $\mathrm{d}S$ with normals $\tilde{v}(\mathbf{x}'')P_j(\mathbf{x}'',\gamma)$ pointing inside. Let us emphasize that the back–propagated infinitesimal Green tensor (16) is no further causal.

Inserting (15) for the Green tensor and using identity

$$\tilde{c}_{njkl}(\mathbf{x}'')E_n(\mathbf{x}'',\gamma)P_j(\mathbf{x}'',\gamma)E_k(\mathbf{x}'',\gamma)P_l(\mathbf{x}'',\gamma) = \tilde{\varrho}(\mathbf{x}'')\ , \qquad (17)$$

equation (16) reads

$$\mathrm{d}G_{im}(\mathbf{x},t,\mathbf{x}',t') \approx \mathrm{d}\Gamma\int \mathrm{d}t''\,\frac{E_i(\mathbf{x},\gamma)E_m(\mathbf{x}',\gamma)T(\mathbf{x}'',\mathbf{x})T(\mathbf{x}'',\mathbf{x}')}{[4\pi]^2\sqrt{\tilde{\varrho}(\mathbf{x})[\tilde{v}(\mathbf{x})]^3\,\tilde{\varrho}(\mathbf{x}')[\tilde{v}(\mathbf{x}')]^3}}$$
$$\times\Big[\delta(t''-\tau(\mathbf{x}'',\mathbf{x})-t)\,\dot{\delta}(t''-\tau(\mathbf{x}'',\mathbf{x}')-t') - \dot{\delta}(t''-\tau(\mathbf{x}'',\mathbf{x})-t)\,\delta(t''-\tau(\mathbf{x}'',\mathbf{x}')-t')\Big]\ , \qquad (18)$$

which may be integrated over t'' to yield

$$\mathrm{d}G_{im}(\mathbf{x},t,\mathbf{x}',t') \approx \mathrm{d}\Gamma\ \frac{E_i(\mathbf{x},\gamma)E_m(\mathbf{x}',\gamma)T(\mathbf{x}'',\mathbf{x})T(\mathbf{x}'',\mathbf{x}')}{[4\pi]^2\sqrt{\tilde{\varrho}(\mathbf{x})[\tilde{v}(\mathbf{x})]^3\,\tilde{\varrho}(\mathbf{x}')[\tilde{v}(\mathbf{x}')]^3}}$$
$$\times\ 2\ \dot{\delta}(t+\tau(\mathbf{x}'',\mathbf{x})-\tau(\mathbf{x}'',\mathbf{x}')-t')\quad . \qquad (19)$$

In the vicinity of point $\mathbf{x}'$, the first–order paraxial approximation of the infinitesimal Green tensor (19), back–propagated from the ray tube of angular size $\mathrm{d}\Gamma$, is

$$\mathrm{d}G_{im}(\mathbf{x},t,\mathbf{x}',t') \approx -\mathrm{d}\Gamma\ \frac{E_i(\mathbf{x}',\gamma)E_m(\mathbf{x}',\gamma)[T(\mathbf{x}'',\mathbf{x}')]^2}{8\pi^2\,\tilde{\varrho}(\mathbf{x}')[\tilde{v}(\mathbf{x}')]^3}\ \dot{\delta}(t'-P_k(\mathbf{x}',\gamma)[x_k-x'_k]-t)\ , \qquad (20)$$

which is, except for the reciprocal transmission coefficient $T(\mathbf{x}'',\mathbf{x}')$ between target point $\mathbf{x}'$ and receiver point $\mathbf{x}''$, independent of $\mathbf{x}''$. The whole back–propagated Green tensor is then

$$G_{im}(\mathbf{x},t,\mathbf{x}',t') = \int_\Gamma \mathrm{d}G_{im}(\mathbf{x},t,\mathbf{x}',t')\ a(\mathbf{x}'')\quad , \qquad (21)$$

where the weighting factor of $a(\mathbf{x}'')$ is inserted to account for possible windowing of the seismic records (time sections) at receiver points $\mathbf{x}''$. The back–propagated scattered wavefield $U_i(\mathbf{x},t)$ may be obtained from equation (14) by means of substituting (21) together with (20) for the Green tensor $\tilde{G}_{im}(\mathbf{x},t,\mathbf{x}',t')$,

$$U_i(\mathbf{x},t) \approx -\int\!\mathrm{d}\mathbf{x}'\!\int\!\mathrm{d}t'\!\int_\Gamma\!\mathrm{d}\Gamma\ A(\mathbf{x}',\gamma)\ \frac{E_i(\mathbf{x}',\gamma)E_m(\mathbf{x}',\gamma)}{8\pi^2\tilde{\varrho}(\mathbf{x}')[\tilde{v}(\mathbf{x}')]^3}$$

$$\times\big[\Delta\varrho(\mathbf{x}')\dot{\tilde{u}}_m(\mathbf{x}',t') - P_j(\mathbf{x}',\gamma)\Delta c_{mjkl}(\mathbf{x}')\tilde{u}_{k,l}(\mathbf{x}',t')\big]\ \ddot{\delta}(t'-P_k(\mathbf{x}',\gamma)[x_k-x'_k]-t)\ , \quad (22)$$

where the partial derivatives are related to variables $\mathbf{x}'$ and t'. Here the "aperture weighting function"

$$\begin{aligned}\gamma\in\Gamma:\quad & A(\mathbf{x}',\gamma) = a(\mathbf{x}'')\ [T(\mathbf{x}'',\mathbf{x}')]^2\\ \gamma\notin\Gamma:\quad & A(\mathbf{x}',\gamma) = 0 \quad ,\end{aligned} \qquad (23)$$

accounts both for the aperture limitation to directions $\gamma\in\Gamma$, for possible windowing $a(\mathbf{x}'')$ of the seismic records (time sections) at receiver points $\mathbf{x}''$, and for the two–way accumulated reciprocal transmission coefficient between target point $\mathbf{x}'$ and receiver point $\mathbf{x}''$. Integration over Γ in (22) and subsequent equations may thus be extended to the whole solid angle (all directions). After time integration, equation (22) reads

$$U_i(\mathbf{x},t) \approx -\!\int\!\mathrm{d}\mathbf{x}'\!\int_\Gamma\!\mathrm{d}\Gamma\ A(\mathbf{x}',\gamma)\ \frac{E_i(\mathbf{x}',\gamma)E_m(\mathbf{x}',\gamma)}{8\pi^2\tilde{\varrho}(\mathbf{x}')[\tilde{v}(\mathbf{x}')]^3}$$

$$\times\Big[\Delta\varrho(\mathbf{x}')\dddot{\tilde{u}}_m(\mathbf{x}',t+P_k(\mathbf{x}',\gamma)[x_k-x'_k]) - P_j(\mathbf{x}',\gamma)\Delta c_{mjkl}(\mathbf{x}')\ddot{\tilde{u}}_{k,l}(\mathbf{x}',t+P_k(\mathbf{x}',\gamma)[x_k-x'_k])\Big]\ . \quad (24)$$

Assuming locally the first–order paraxial approximation

$$\tilde{u}_k(\mathbf{x},t) \approx e_k(\mathbf{x}')f\,(t-p_k(\mathbf{x}')[x_k-x'_k]) \qquad (25)$$

of the incident wave, centred at $\mathbf{x}'$, equation (24) reads

$$U_i(\mathbf{x},t) \approx -\int\!\mathrm{d}\mathbf{x}'\int_\Gamma\!\mathrm{d}\Gamma\ A(\mathbf{x}',\gamma)\ \frac{E_i(\mathbf{x}',\gamma)}{4\pi^2[\tilde{v}(\mathbf{x}')]^3}\ r(\mathbf{x}',\gamma)\ \dddot{f}(t+P_k(\mathbf{x}',\gamma)[x_k-x'_k])\ , \qquad (26)$$

where

$$\boxed{r(\mathbf{x}',\gamma) = \frac{\Delta\varrho(\mathbf{x}')E_m(\mathbf{x}',\gamma)e_m(\mathbf{x}') + \Delta c_{mjkl}(\mathbf{x}')E_m(\mathbf{x}',\gamma)P_j(\mathbf{x}',\gamma)e_k(\mathbf{x}')p_l(\mathbf{x}')}{2\ \tilde{\varrho}(\mathbf{x}')} \qquad (27)}$$

is the angle–dependent "reflectivity function".

Here the angular dependence of $\dddot{f}(t+P_k(\mathbf{x}',\gamma)[x_k-x'_k])$ is essential because it controls the space–time distribution of the back–propagated scattered wavefield $U_i(\mathbf{x},t)$. On the other hand, the angular dependence of $E_m(\mathbf{x}',\gamma)e_m(\mathbf{x}')$ corresponds to the cosine between the two vectors and the angular dependence of $\Delta c_{mjkl}(\mathbf{x}')E_m(\mathbf{x}',\gamma)P_j(\mathbf{x}',\gamma)$ $\times e_k(\mathbf{x}')p_l(\mathbf{x}')$ very roughly corresponds to a product of two cosines which should not be more rapidly changing than $\cos^2$. We may thus often substitute $E_k(\mathbf{x}',\gamma)$ and $P_j(\mathbf{x}',\gamma)$ in the reflectivity function with their mean values $\overline{E}_k(\mathbf{x}')$ and $\overline{P}_k(\mathbf{x}')$ over the aperture Γ,

$$U_i(\mathbf{x},t) \approx -\int\!\mathrm{d}\mathbf{x}'\,\frac{\overline{E}_i(\mathbf{x}')}{\pi[\tilde{v}(\mathbf{x}')]^3}\ \overline{r}(\mathbf{x}')\ \int_\Gamma\!\mathrm{d}\Gamma\ \frac{A(\mathbf{x}',\gamma)}{4\pi}\ \dddot{f}(t+P_k(\mathbf{x}',\gamma)[x_k-x'_k])\ , \qquad (28)$$

where

$$\boxed{\overline{r}(\mathbf{x}') = \frac{\Delta\varrho(\mathbf{x}')\overline{E}_m(\mathbf{x}')e_m(\mathbf{x}') + \Delta c_{mjkl}(\mathbf{x}')\overline{E}_m(\mathbf{x}')\overline{P}_j(\mathbf{x}')e_k(\mathbf{x}')p_l(\mathbf{x}')}{2\ \tilde{\varrho}(\mathbf{x}')} \qquad (29)}$$

is the angle–independent reflectivity function. The relative error of this substitution with respect to the peak value of the reflectivity function should not exceed $(\Delta\gamma)^2/12$, where $\Delta\gamma$ is the maximum diameter of the aperture Γ measured in radians.

5 Examples of reflectivity functions

5.1 Backward (zero–offset) and forward scattering

All backward (zero–offset) reflectivity functions ($P_k = p_k$), without conversion between polarizations, are

$$r_{\text{backward}} = \frac{\Delta v}{\tilde{v}} + \frac{\Delta\varrho}{\tilde{\varrho}} \quad , \tag{30}$$

where the polarization vectors of incident and back–propagated scattered waves are assumed to coincide ($E_k = e_k$). All forward reflectivity functions ($P_k = -p_k$), without conversion, are

$$r_{\text{forward}} = -\frac{\Delta v}{\tilde{v}} \quad , \tag{31}$$

where, unlike as in equations (37) and (41) below, the polarization vectors of incident and scattered waves are assumed to coincide ($E_k = e_k$). Forward reflectivity (31) just corresponds to a linearized travel–time perturbation (Woodward & Rocca 1988; Coates & Chapman 1990; Woodward 1992; Pratt et al. 1994; Priolo, Chiaruttini & Pregarz 1996) not resolved by migrations.

5.2 Reflectivity functions in an isotropic medium

For example, in a case of an isotropic perturbation

$$\Delta c_{ijkl} = \Delta\lambda\delta_{ij}\delta_{kl} + \Delta\mu\,[\delta_{ik}\delta_{jl} + \delta_{il}\delta_{jk}] \tag{32}$$

to the isotropic model

$$\tilde{c}_{ijkl} = \tilde{\lambda}\delta_{ij}\delta_{kl} + \tilde{\mu}\,[\delta_{ik}\delta_{jl} + \delta_{il}\delta_{jk}] \quad , \tag{33}$$

the reflectivity function simplifies to read

$$r = \frac{\Delta\varrho}{2\tilde{\varrho}}E_m e_m + \frac{\Delta\lambda E_m P_m e_k p_k + \Delta\mu[E_m e_m P_k p_k + E_m p_m P_k e_k]}{2\ \tilde{\varrho}} \quad . \tag{34}$$

We define

$$\cos(2\theta) = P_k p_k [P_m P_m]^{-\frac{1}{2}}[p_n p_n]^{-\frac{1}{2}} \quad , \qquad \sin(2\theta) = \pm\sqrt{1 - [\cos(2\theta)]^2} \quad , \tag{35}$$

where the $\pm$ sign depends on the S-wave polarization and affects only P-SV and SV-P reflectivity functions. Without conversion, the polarization vectors of incident and back–propagated waves are assumed to coincide for zero–offset rays.

The P-P reflectivity function is then

$$r_{\text{P-P}} = \frac{\Delta\varrho}{2\tilde{\varrho}}\cos(2\theta) + \frac{\Delta\lambda + 2\Delta\mu\ [\cos(2\theta)]^2}{2[\tilde{\lambda} + 2\ \tilde{\mu}]} \quad , \tag{36}$$

i.e.,

$$r_{\text{P-P}} = \frac{\Delta v_P}{\tilde{v}_P} - 2\left[\frac{\tilde{v}_S}{\tilde{v}_P}\right]^2 [\sin(2\theta)]^2 \frac{\Delta v_S}{\tilde{v}_S} + \left[1 + \cos(2\theta) - 2\left(\frac{\tilde{v}_S}{\tilde{v}_P}\right)^2 [\sin(2\theta)]^2\right] \frac{\Delta\varrho}{2\tilde{\varrho}} \ . \quad (37)$$

The P-SV and SV-P reflectivity functions are

$$r_{\text{P-SV}} = \frac{\Delta\varrho}{2\tilde{\varrho}} \sin(2\theta) + \frac{\Delta\mu \sin(2\theta)\cos(2\theta)}{\sqrt{\tilde{\mu}\ [\tilde{\lambda} + 2\tilde{\mu}]}} \quad , \quad (38)$$

i.e.,

$$r_{\text{P-SV}} = 2\sin(2\theta)\cos(2\theta)\frac{\tilde{v}_S}{\tilde{v}_P}\frac{\Delta v_S}{\tilde{v}_S} + \sin(2\theta)\left[\frac{1}{2} + \cos(2\theta)\frac{\tilde{v}_S}{\tilde{v}_P}\right]\frac{\Delta\varrho}{\tilde{\varrho}} \quad . \quad (39)$$

The SV-SV reflectivity function is

$$r_{\text{SV-SV}} = \frac{\Delta\varrho}{2\tilde{\varrho}}\cos(2\theta) + \frac{\Delta\mu\ \left[[\cos(2\theta)]^2 - [\sin(2\theta)]^2\right]}{2\ \tilde{\mu}} \quad , \quad (40)$$

i.e.,

$$r_{\text{SV-SV}} = \left[[\cos(2\theta)]^2 - [\sin(2\theta)]^2\right]\frac{\Delta v_S}{\tilde{v}_S} + \frac{\cos(2\theta) + [\cos(2\theta)]^2 - [\sin(2\theta)]^2}{2}\frac{\Delta\varrho}{\tilde{\varrho}} \ . \quad (41)$$

The SH-SH reflectivity function is

$$r_{\text{SH-SH}} = \frac{\Delta\varrho}{2\tilde{\varrho}} + \frac{\Delta\mu\ \cos(2\theta)}{2\ \tilde{\mu}} \quad , \quad (42)$$

i.e.,

$$r_{\text{SH-SH}} = \cos(2\theta)\frac{\Delta v_S}{\tilde{v}_S} + \frac{1 + \cos(2\theta)}{2}\frac{\Delta\varrho}{\tilde{\varrho}} \quad . \quad (43)$$

6 Explicit forms of the imaging functional

It is natural to assume the imaging functional (9) invariant with respect to shift in time, and linear with respect to the second argument representing the back–propagated scattered wavefield (Claerbout 1971). In addition, the imaging functional should be a homogeneous function of the order of -1 with respect to the first argument representing the incident wavefield, in order to preserve the proportionality between the perturbations of material parameters and the migrated section.

The above conditions are satisfied, e.g., by a very broad class of imaging functionals of the form

$$M(\tilde{u}_i, U_i) = \int \mathrm{d}\omega \frac{\widehat{F}(\omega)\widehat{\tilde{u}}_j^*(\omega) E_{jk} \widehat{U}_k(\omega)}{\widehat{\tilde{u}}_m^*(\omega) e_{mn} \widehat{\tilde{u}}_n(\omega)} \left[\int \mathrm{d}\omega \widehat{F}(\omega)\right]^{-1} \quad , \quad (44)$$

which is the elastic analogy to the scalar imaging functionals by, e.g., Claerbout (1971) eq. (3), or Scales (1995) eq. (4). Here the frequency range of user–defined spectral filter $\widehat{F}(\omega)$ should not exceed the frequency range of $\widehat{\tilde{u}}_i(\omega)$ and matrices $E_{jk} = E_{jk}(\mathbf{x}')$ and $e_{jk} = e_{jk}(\mathbf{x}')$ should depend on slowness vectors $p_m(\mathbf{x}')$ and $\overline{P}_m(\mathbf{x}')$ in such a way to approximately decompose both the incident and back–propagated scattered wavefields into P and two S wave polarizations,

$$E_{jk}(\mathbf{x}') = e_j(\mathbf{x}')\overline{E}_k(\mathbf{x}') \ , \quad e_{jk}(\mathbf{x}') = e_j(\mathbf{x}')e_k(\mathbf{x}') \quad (45)$$

for a particular pair of polarizations. Note that not all 9 pairs should always be considered. For instance, P-SH, SV-SH, SH-P and SH-SV scattering should be small for isotropic perturbations to isotropic macro–model. Here SV and SH are considered with respect to the plane given by slowness vectors $p_m(\mathbf{x}')$ and $\overline{P}_m(\mathbf{x}')$.

For

$$\widehat{F}(\omega) = \widehat{\tilde{u}}^*_m(\omega) e_{mn} \widehat{\tilde{u}}_n(\omega) \quad , \tag{46}$$

the convolutional functional is obtained, see, e.g., Claerbout (1971) eq. (4), Stolt & Benson (1986) eq. (5.107). However, in a presence of multiples in the approximation $\tilde{u}_i(t)$ of the incident wavefield, $\widehat{\tilde{u}}_i(\omega)$ in (46) should be replaced by function $\widehat{s}(\omega)$ close to the Fourier transform of the source time function corrected for the attenuation,

$$\widehat{F}(\omega) = \widehat{s}^*(\omega) \widehat{s}(\omega) \quad . \tag{47}$$

The image corresponding to (47) may probably further be sharpened by the choice of

$$\widehat{F}(\omega) = |\widehat{s}(\omega)| \quad . \tag{48}$$

Since the decomposition into P and S waves enabled by the zero–derivative imaging functionals (44) is very rough, the first–derivative imaging functionals

$$M(\tilde{u}_i, U_i) = \int \mathrm{d}\omega \, \frac{\widehat{F}(\omega) \widehat{\tilde{u}}^*_{i,j}(\omega) E_{ijkl} \widehat{U}_{k,l}(\omega)}{\widehat{\tilde{u}}^*_{m,r}(\omega) e_{mrns} \widehat{\tilde{u}}_{n,s}(\omega)} \left[\int \mathrm{d}\omega \, \widehat{F}(\omega) \right]^{-1} \tag{49}$$

may be introduced. In isotropic macro–models, we may choose

$$E_{ijkl}(\mathbf{x}') = e_{ij}(\mathbf{x}') \overline{E}_{kl}(\mathbf{x}') \quad , \qquad e_{ijkl}(\mathbf{x}') = e_{ij}(\mathbf{x}') e_{kl}(\mathbf{x}') \tag{50}$$

with

$$E_{ij}(\mathbf{x}') = \delta_{ij} \tilde{v}_P(\mathbf{x}') \ , \quad e_{ij}(\mathbf{x}') = \delta_{ij} \tilde{v}_P(\mathbf{x}') \tag{51}$$

for P waves and

$$\begin{aligned} E_{ij}(\mathbf{x}') &= [E_i(\mathbf{x}') \overline{P}_j(\mathbf{x}') - E_j(\mathbf{x}') \overline{P}_i(\mathbf{x}')][\tilde{v}_S(\mathbf{x}')]^2 \quad , \\ e_{ij}(\mathbf{x}') &= [e_i(\mathbf{x}') p_j(\mathbf{x}') - e_j(\mathbf{x}') p_i(\mathbf{x}')][\tilde{v}_S(\mathbf{x}')]^2 \end{aligned} \tag{52}$$

for S waves.

7 Analysis of the migrated section

Assume the imaging functional (9) invariant with respect to shift in time, and linear with respect to the second argument representing the back–propagated scattered wavefield. The "imaging function"

$$\Phi(\Delta t) = M\big(e_i(\mathbf{x}') f(\bullet), \overline{E}_i(\mathbf{x}') f(\bullet + \Delta t)\big) \tag{53}$$

may then be defined in terms of the imaging functional and the local "time function" $f(t)$. For the imaging functional in the form of (44) with (45), or (49) with (50)–(52),

$$\Phi(\Delta t) \approx \frac{F(\Delta t)}{F(0)} \quad . \tag{54}$$

The "resolution function"

$$S(\mathbf{x}', \mathbf{x} - \mathbf{x}') = - \int_\Gamma \mathrm{d}\Gamma \, \frac{A(\mathbf{x}',\gamma)}{[2\pi]^2 [\tilde{v}(\mathbf{x}')]^3} \; \dddot{\Phi}([P_k(\mathbf{x}',\gamma) + p_k(\mathbf{x}')][x_k - x'_k]) \tag{55}$$

may then be defined in terms of the imaging function $\Phi(\Delta t)$, see (25) and (28).

The *migrated section* has then the form of integral operator

$$\boxed{m(\mathbf{x}) \approx \int \mathrm{d}\mathbf{x}' \; S(\mathbf{x}', \mathbf{x}-\mathbf{x}') \; \overline{r}(\mathbf{x}') \quad . \qquad (56)}$$

which has locally the character of convolution because the resolution function $S(\mathbf{x}', \mathbf{x}–\mathbf{x}')$ depends firstly on vector $\mathbf{x}-\mathbf{x}'$ and is just moderately varying with the location $\mathbf{x}'$.

We may write

$$\ddot{\Phi}(\Delta t) = -\int \mathrm{d}\omega \; \omega^2 \frac{\widehat{\dot{\Phi}}(\omega)}{2\pi \; \widehat{\delta}(\omega)} \exp(-\mathrm{i}\omega\Delta t) \tag{56a}$$

and, consequently,

$$S(\mathbf{x}', \mathbf{x}-\mathbf{x}') = \int_{\Gamma} \mathrm{d}\Gamma \int \mathrm{d}\omega \; \omega^2 \frac{A(\mathbf{x}',\gamma) \; \widehat{\dot{\Phi}}(\omega)}{[2\pi]^3 [\tilde{v}(\mathbf{x}')]^3 \widehat{\delta}(\omega)} \exp(-\mathrm{i}\omega[P_k(\mathbf{x}',\gamma)+p_k(\mathbf{x}')][x_k-x'_k]) \; . \tag{56b}$$

If we introduce wavenumbers

$$k_i = \omega[P_i(\mathbf{x}',\gamma) + p_i(\mathbf{x}')] \quad , \tag{56c}$$

the Jacobian of the corresponding transformation is

$$\frac{\mathrm{d}\mathbf{k}}{\mathrm{d}\Gamma \mathrm{d}\omega} = \frac{\omega^2}{[\tilde{v}(\mathbf{x}')]^2} |\mathbf{P}(\mathbf{x}',\gamma) + \mathbf{p}(\mathbf{x}')| \; \cos(\Theta) \quad , \tag{56d}$$

where

$$\cos(\Theta) = \frac{[P_k(\mathbf{x}',\gamma) + p_k(\mathbf{x}')] P_k(\mathbf{x}',\gamma)}{|\mathbf{P}(\mathbf{x}',\gamma) + \mathbf{p}(\mathbf{x}')||\mathbf{P}(\mathbf{x}',\gamma)|} \tag{56e}$$

may be called the cosine of the reflection angle.

Inserting equations ($56c, d, e$) into ($56b$), we see that the 3-D Fourier transform of the resolution function (55) with respect to $\mathbf{x} - \mathbf{x}'$ may be expressed in the form of

$$\widehat{S}(\mathbf{x}', \mathbf{k}) = W(\mathbf{x}', \mathbf{k}) \; \widehat{\delta}(\mathbf{k}) \quad , \tag{57}$$

where the 3-D Fourier transform $\widehat{\delta}(\mathbf{k})$ of the 3-D Dirac distribution $\delta(\mathbf{x})$ is filtered with the wavenumber filter $W(\mathbf{x}', \mathbf{k})$,

$$W(\mathbf{x}', [\mathbf{p}(\mathbf{x}') + \mathbf{P}(\mathbf{x}',\gamma)]\omega) = \frac{A(\mathbf{x}',\gamma) \; \widehat{\dot{\Phi}}(\omega)}{\tilde{v}(\mathbf{x}') \; |\mathbf{p}(\mathbf{x}') + \mathbf{P}(\mathbf{x}',\gamma)| \; \widehat{\delta}(\omega) \cos(\Theta)} \quad , \tag{58}$$

specified in terms of the 1-D fourier transforms of the 1-D Dirac distribution $\delta(\Delta t)$ and the derivative $\dot{\Phi}(\Delta t)$ of the imaging function.

Replacing $\widehat{\dot{\Phi}}(\omega)$ on the right–hand side of (58) by $-\mathrm{i}k_k \frac{[P_k(\mathbf{x}',\gamma)+p_k(\mathbf{x}')]}{|\mathbf{P}(\mathbf{x}',\gamma)+\mathbf{p}(\mathbf{x}')|^2} \widehat{\Phi}(\omega)$ and approximating $\mathbf{p}(\mathbf{x}') + \mathbf{P}(\mathbf{x}',\gamma)$ by $\mathbf{p}(\mathbf{x}') + \overline{\mathbf{P}}(\mathbf{x}')$, which is analogous to approximating reflectivity $r(\mathbf{x}',\gamma)$ by $\overline{r}(\mathbf{x}')$, we may introduce considerably simplified wavenumber filter

$$w(\mathbf{x}', [\mathbf{p}(\mathbf{x}') + \mathbf{P}(\mathbf{x}',\gamma)]\omega) = \frac{A(\mathbf{x}',\gamma) \; \widehat{\Phi}(\omega)}{|\mathbf{p}(\mathbf{x}') + \mathbf{P}(\mathbf{x}',\gamma)| \; \widehat{\delta}(\omega)} \tag{59}$$

and express the migrated section in the form of

$$\boxed{m(\mathbf{x}) \approx \int \mathrm{d}\mathbf{x}' \; s(\mathbf{x}', \mathbf{x}-\mathbf{x}') \; \overline{R}(\mathbf{x}') \quad , \qquad (60)}$$

where

$$\widehat{s}(\mathbf{x}', \mathbf{k}) = w(\mathbf{x}', \mathbf{k}) \; \widehat{\delta}(\mathbf{k}) \tag{61}$$

and

$$\overline{R}(\mathbf{x}') = \frac{\overline{r}_{,k}(\mathbf{x}') \; [p_k(\mathbf{x}') + \overline{P}_k(\mathbf{x}')]}{\tilde{v}(\mathbf{x}') \; |\mathbf{p}(\mathbf{x}') + \overline{\mathbf{P}}(\mathbf{x}')|^2 \; \cos(\Theta)} \tag{62}$$

is the spatial distribution of the reflection coefficient.

For example, in a case of a single plane interface $x_3 = 0$ between two homogeneous materials and scattering into the direction corresponding to Snell's law, the spatial distribution of the reflection coefficient is $\overline{R}(\mathbf{x}) = R \; \delta(x_3)$, where R is the plane–wave reflection coefficient. Within the Born approximation used throughout this paper, the reflection coefficient R is, naturally, approximation of the plane–wave reflection coefficient (Červený & Ravindra 1971) for very small contrasts of material parameters. For P-P scattering, the reflection coefficient R corresponds to the reflection coefficient of Stolt & Benson (1986) eq. (1.7).

8 Numerical examples

The effect of convolutional filtering (56) to (58) on the structure from Figure 1 is demonstrated in Figures 2 and 3. We may assume, e.g., that the velocities are constant and that Figure 1 displays small density perturbations. Figures 2, 3 and 4 then show the images of the density which can ideally be obtained by seismic migration for a given configuration and source time function.

Acknowledgements

I am indebted to Paul Spudich who provided me with his perfect code I could modify to calculate the numerical examples presented here.

The research has been partially supported by the Grant Agency of the Czech Republic under Contract 205/95/1465, and by the consortium "Seismic Waves in Complex 3-D Structures".

References

Červený, V. & Ravindra, R. (1971): Theory of Seismic Head Waves. Univ. Toronto Press, Toronto.

Coates, R.T. & Chapman, C.H. (1990): Ray perturbation theory and the Born approximation. Geophys. J. int., **100**, 379–392.

Claerbout, J.F. (1971): Toward a unified theory of reflector mapping. Geophysics, **36**, 467–481.

Pratt, R.G., Song, Z.-M., Williamson, P. & Warner, M. (1996): Two–dimensional velocity models from wide–angle seismic data by wavefield inversion. Geophys. J. int., **124**, 323–340.

Priolo, E., Chiaruttini, C. & Pregarz, A. (1996): Analytical and numerical analysis of tomographic resolution with bandlimited signals. Geophysics, submitted.

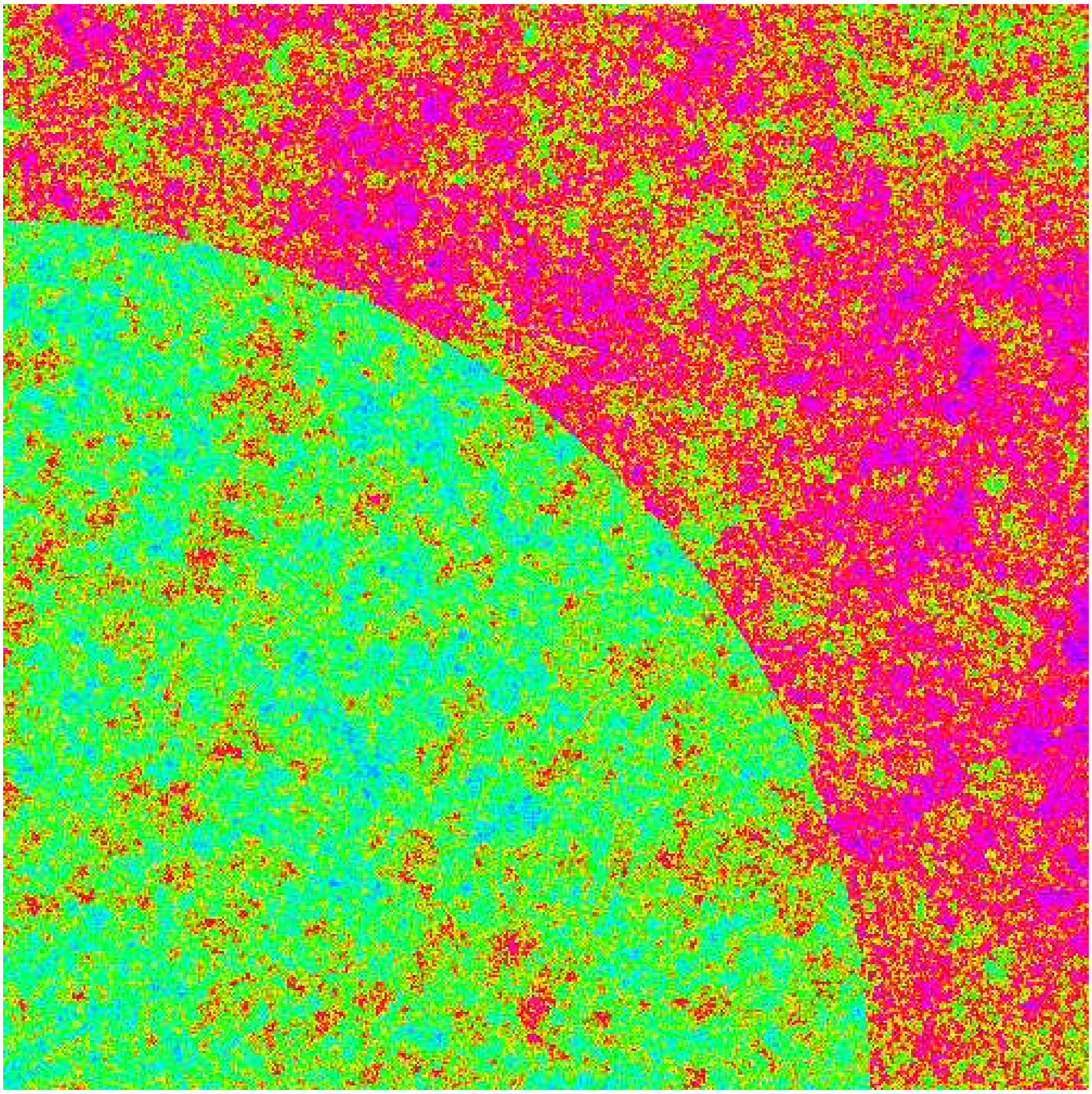

Figure 1. Structure of the target zone. Randomly generated representation of the self–affine medium is superposed with a homogeneous quarter circle in order to supplement random heterogeneities with a sharp interface. The target zone is assumed small compared with its depth below the source and receivers.

Scales, J.A. (1995): Theory of Seismic Imaging. (Lecture Notes in Earth Sciences, Vol. 55), Springer, Berlin–Heidelberg.

Stolt, R.H. & Benson, A.K. (1986): Seismic Migration. Theory and Practice. (Handbook of Geophysical Exploration, Section I: Seismic Exploration, Vol. 5), Geophysical Press, London–Amsterdam.

Woodward, M.J. & Rocca, F. (1988): Wave–equation tomography. Expanded Abstracts of 58th Annual Int. SEG Meeting (Anaheim), 1232–1235, Soc. Exploration Geo-

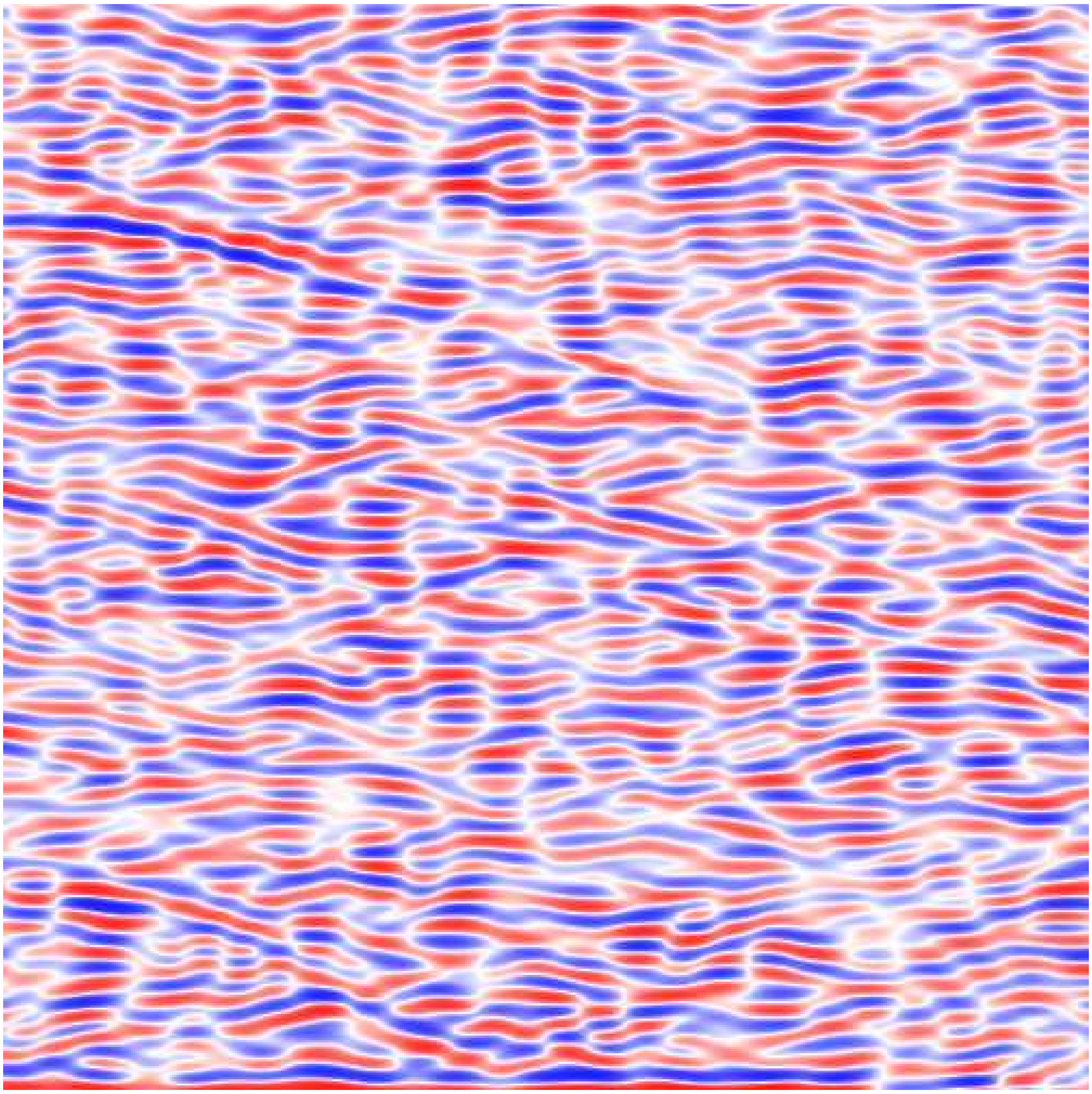

Figure 2. Common–source prestack migrated section of the structure displayed in Figure 1, simulated according to equations (56) to (58) in a homogeneous macro–model. Imaging function is the Gabor signal with the predominant wavelength of 6% the target zone dimension. Length of the symmetric receiver profile, with the source above the target zone (angle 0°), is twice the depth of the target zone, which corresponds to aperture from -45° to 45°. Only wavenumber vectors between -22.5° and 22.5° are thus present in the image.

physicists, Tulsa.
Woodward, M.J. (1992): Wave–equation tomography. Geophysics, **57**, 15–26.

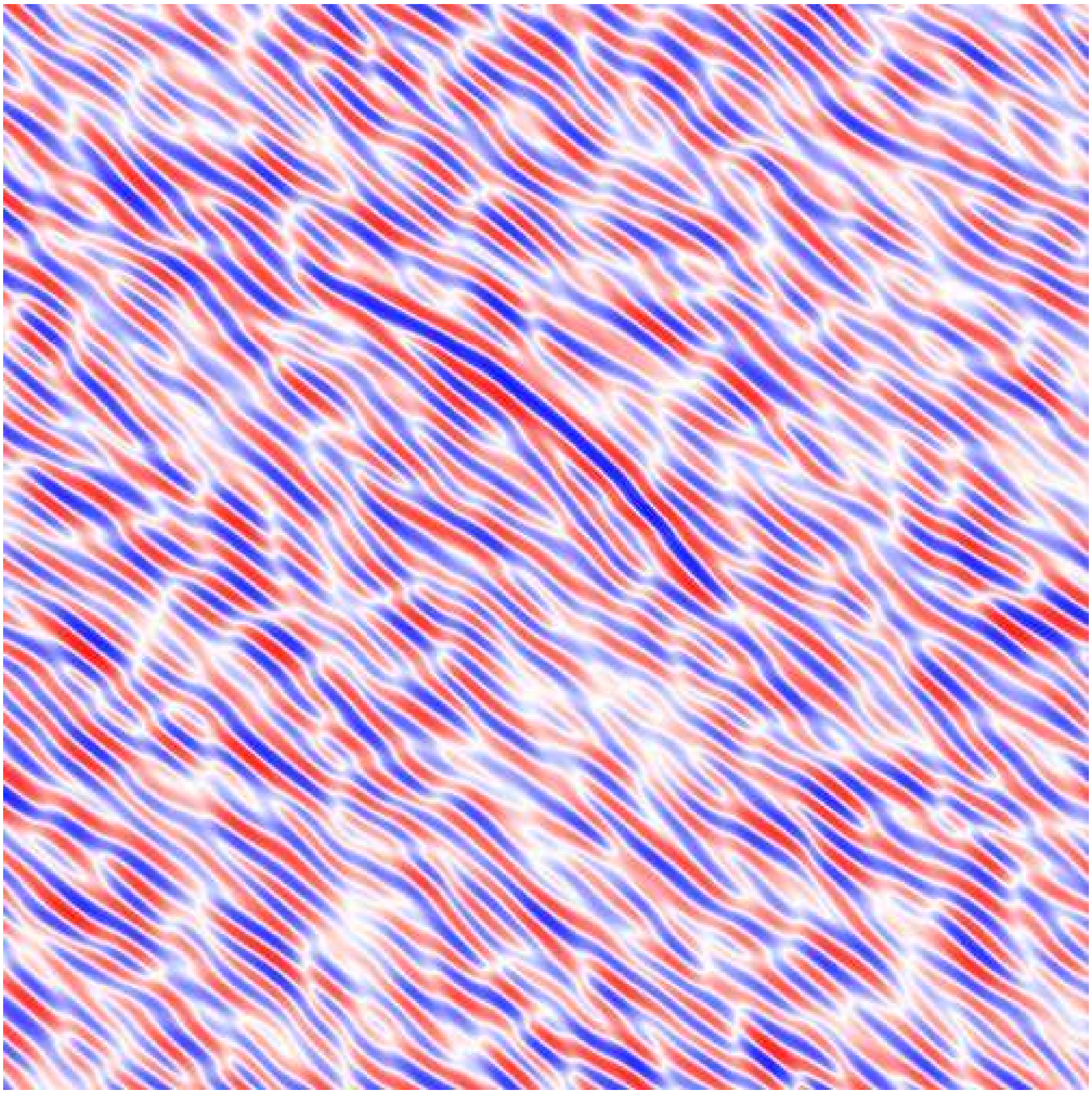

Figure 3. Common–source prestack migrated section of the structure displayed in Figure 1, simulated according to equations (56) to (58) in a homogeneous macro–model. The symmetric receiver profile from Figure 2 has been shifted to the right, locating the leftmost receiver above the target zone. The source is thus in the direction of 45° and the aperture extends from 0° to 63°. Only wavenumber vectors between 22.5° and 54° are thus present in the image.

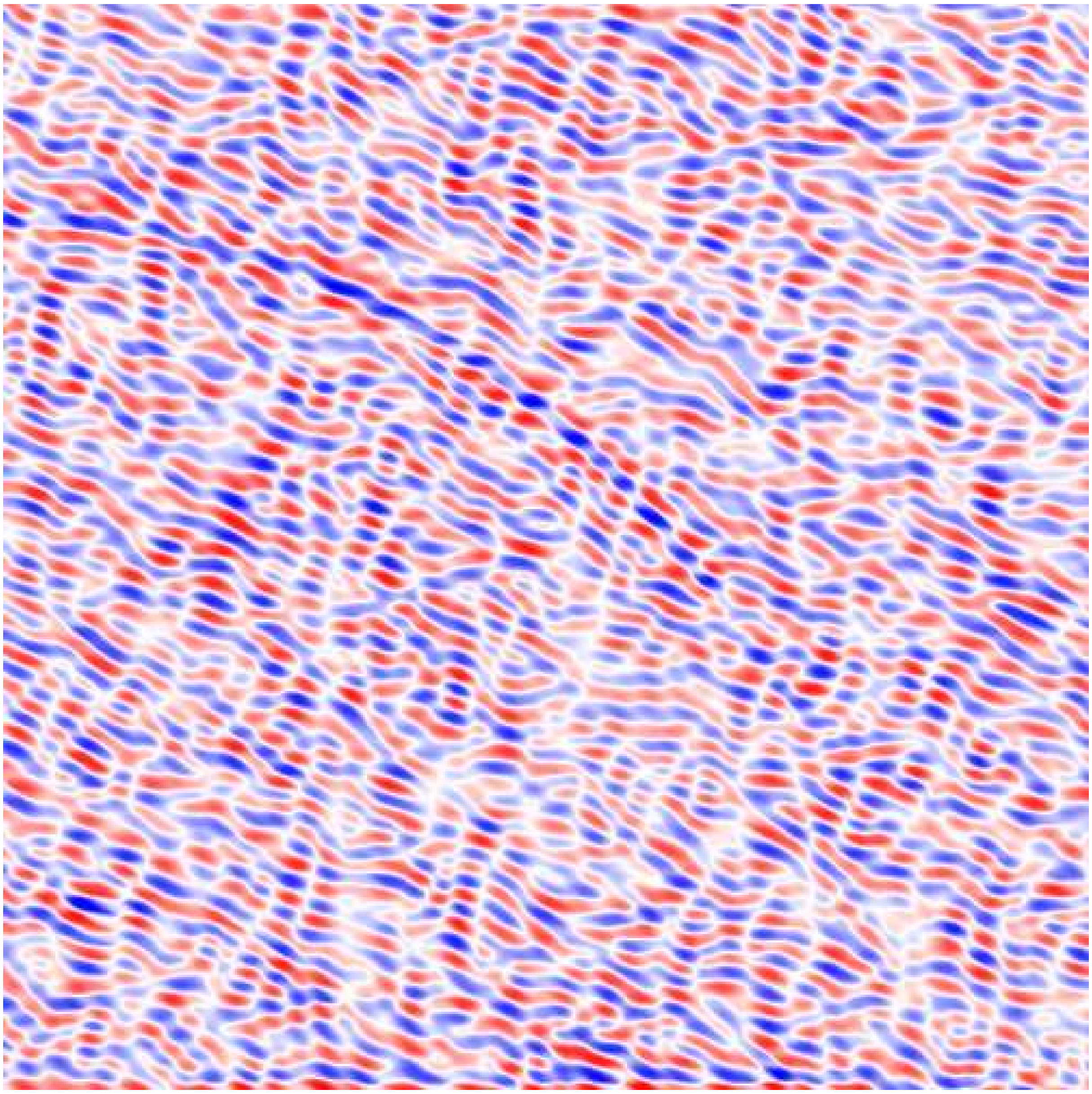

Figure 4. Sum of the common–source prestack migrated sections of Figures 2 and 3. Let us emphasize that Figures 2, 3 and 4 are not a result of a particular migration, they show which features of the structure can be resolved by an ideal migration (no multiples, no noise, no transmission losses, perfect macro–model, exact calculation of elastic wavefields).